



## Analysis of Surface Wave Attenuation in Mangrove Forests

Safwan Hadi<sup>1)</sup>, Hamzah Latief<sup>1)</sup> & Muliddin<sup>2)</sup>

<sup>1)</sup> Study Program of Oceanography, Institut Teknologi Bandung

<sup>2)</sup> Physics Dept. Halu Oleo University

**Abstract.** This paper presents an analytical study on surface wave attenuation in mangrove forest using analytical model developed by Massel et.al. (1999). The energy dissipation in the frequency domain is determined by treating the mangrove forest as a random media with certain characteristics using the geometry of mangrove trunks and their locations. Initial nonlinear governing equations are linearized using the concept of minimalization in the stochastic sense and interactions between mangrove trunks and roots have been introduced through the modification of the drag coefficients. To see the effectiveness of the mangrove forest in attenuating wave energy the analytical model was applied to two types of mangrove forest i.e. *Rhizophora* and *Ceriops* forests. The resulting rate of wave energy attenuation depends strongly on the density of the mangrove forest, and on diameter of mangrove roots and trunks. More effective wave energy attenuation is shown by *Rhizophora*.

**Keywords:** *analytical model; mangrove; wave attenuation.*

### 1 Introduction

Mangroves are densely vegetated mudflats that exist at the boundary of marine and terrestrial environments. Inherent in this habitat is their ability to survive in a highly saline environment (Robertson and Alongi, 1992 in Massel et.al, 1999). In recent years it has been realized that mangroves may have a special role in supporting fisheries, stabilizing the coastal zone and protecting the lives and properties of the people living near the sea and offshore islands (Jackson and Winant, 1983; Jenkins and Skelly, 1987; Qureshi, 1990; Siddiqi and Khan, 1990; Mazda et al., 1997a in Massel et.al, 1999). Experimental and numerical works on the effect of mangrove in reducing tsunami's impact have been done by Latief (2000) and Latief et. al (2000).

Hydrodynamic factor play a major role in the structure and function of mangrove ecosystems. Biogeochemical and trophodynamic processes, and forest structure and growth are intimately linked to water movement. However, studies of physical processes in tropical mangrove swamps and mangrove-fringed estuaries are few, and far behind compared to those of temperate estuaries. Water circulation in riverine mangrove forests, which comprises tidal

creeks and shallow mangrove swamps, has been studied somewhat more than the other types of mangrove forests (Wolanski et al., 1992 in Massel et al., 1999); Furukawa and Wolanski, 1996; Furukawa et al., 1997 in Massel et al., 1999).

Long wave, namely tidal waves, are the dominant cause of water movement and sedimentation in mangrove system. Tidal currents in creeks often exceed 1 m/s, however, velocities within swamps rarely reach 0.1 m/s. Modeling of tidal induced water motion in the mangrove creak is based on vertically averaged, barotropic equation of motion for unsteady flow in open channel with lateral storage in mangrove swamps (Wolanski et al., 1992 in Massel et al., 1999). The problem of parameterization of the friction induced by vegetation is still unsolved.

During the tropical cyclones, however, energy of waves induced by cyclonic winds substantially exceeds tidal energy. Due to the complexity of mangrove systems, the transmission of cyclone-induced waves through mangrove areas is still poorly understood. Assuming that the diameter of particular mangrove trunks is very small in comparison with wavelength, wave energy is dissipated mostly due to drag forces induced on trunks by waves. It should be noted that the number of trunks and their diameters changes with vertical distance from the sea bottom (Mazda et al., 1997b in Massel et al., 1999).

The purpose of the present paper is to do an analytical study on the attenuation of wind induced random surface waves in mangrove forests using the analytical model develop by Massel et al. (1999). Two case studies were investigated in applying the analytical model i.e. wave attenuation in *Rhizophora* forest and in *Ceriops* forest to see the effectiveness of these two species in attenuating waves. A full boundary value problem is solved and the attenuation of the surface waves spectrum is predicted. Waves penetrating through mangrove forest are subject to substantial energy loss. There are two main energy dissipation mechanisms in the mangrove forests: multiple interactions of wave motion with mangrove trunks and roots, and bottom friction. Bottom friction can be accommodated through the concept of a bottom friction coefficient. However, at this stage, the bottom friction will be omitted, as the bottom friction coefficient for mangrove forests is not known.

Mangrove trunks and roots are treated as cylindrical elements located in the water column. In typical mangrove areas, especially occupied by *Rhizophora* species, the density of mangrove trunks and roots is greater in the bottom layer than the upper layer, where only the vertical trunks are observed (Wolanski et al., 1992 in Massel et al., 1999). Wave-induced forces on trunks and roots are

inertial and drag-type forces. For typical mangrove trunks and roots the drag force dominates over inertia forces (Massel et al., 1999).

Because of proximity of other trunks, some interactions between them can be expected. To include these interactions in the resulting drag force, the appropriate modification of the drag coefficient  $C_d$ , depending on the density of the mangrove trunks, was proposed using the discrete vortex method (Kawahara, 1978; Furukawa and Hosokawa, 1996; Hansen and Arneborg, 1997 in Massel et al., 1999).

Sea water is treated as inviscid and incompressible and wave motion is treated as irrotational so that an existence of velocity potential in front of, in, and behind the mangrove forests can be assumed. The velocity potentials in the particular regions are subsequently matched using the boundary conditions. Although the assumption of the potential motion in front and behind the mangrove forest is rather readily acceptable, it is not the case of mangrove forest region. The justification of velocity potential assumption in this region is given in this paper.

## 2 Governing Equations

Let the origin of a rectangular coordinate system  $O(x,z)$  be taken at the mean free surface of the fluid, and the axes be chosen so that the x-coordinate is horizontal and the z-coordinate is vertical and increasing upwards (Fig. 1). A unidirectional random wave train of a given frequency spectrum,  $S(\omega)$ , is normally incident on a mangrove area. The water depth is assumed to be constant and equal to  $h$ . Width of mangrove area is equal to  $l$ .

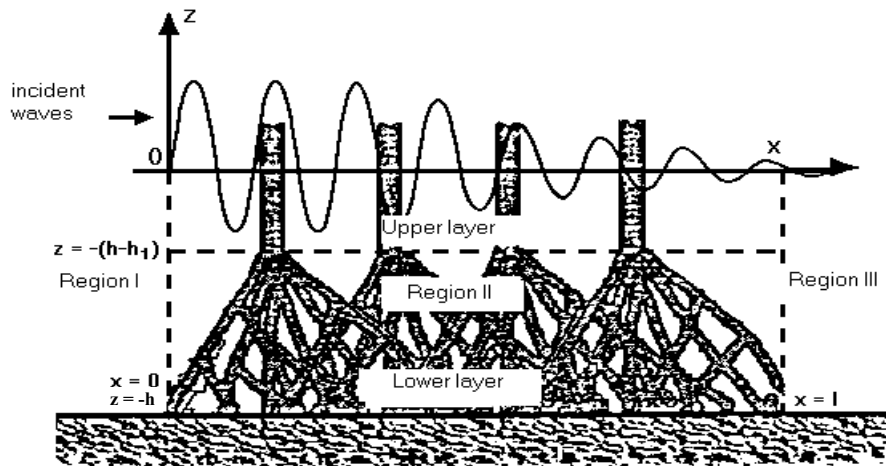


Figure 1 Coordinate system (Massel et. al, 1999).

At the front of the mangrove forest (Region I :  $-\infty < x < 0$ ;  $-h < z < 0$ ) the wave field is composed from incident waves and wave reflected from mangrove forest. The resulting velocity potential takes the form (Massel et al., 1996)

$$\begin{aligned} \Phi_1(x, z, t) = \Re \int_0^{\infty} \left( \frac{-ig}{\omega} \right) \exp(-i\omega t) \\ \times \left\{ [\exp(ikx) - \exp(-ikx)] \frac{\cosh k(z+h)}{\cosh kh} + \sum_{\alpha} M_{\alpha} \exp(\alpha x) \frac{\cos \alpha(z+h)}{\cos \alpha h} \right\} dA_1(\omega) \end{aligned} \quad (1)$$

in which the complex wave number  $\alpha$  must satisfy the following dispersion relation

$$\frac{\omega^2}{g} + \alpha \tan(\alpha h) = 0 \quad (2)$$

Dispersion relation (2) has an infinite discrete set of real roots  $\pm \alpha_n$  and a pair of imaginary roots  $\alpha_0 = \pm ik$ . In our notation, only the positive real roots  $\alpha_n$  and negative imaginary root  $\alpha_0 = -ik$  have a physical sense.

Wave motion within the mangrove forest (Region II :  $0 < x < l$ ;  $-h < z < 0$ ) is subjected to strong dissipation due to the multiple interactions with mangrove trunks and bottom friction. However, in the following, we will concentrate mostly on the interaction of surface waves with mangrove trunks and roots. Hence, the momentum equation for motion with dissipation can be written as follows

$$\frac{\partial \bar{u}_2}{\partial t} = -\frac{1}{\rho} \nabla(p_2 + \rho g z) - \frac{1}{\rho} \bar{F} \quad (3)$$

in which  $\bar{u}_2 = (u_2, w_2)$  is the wave-induced velocity vector in Region II,  $p_2$  is the corresponding dynamic pressure and  $\bar{F}$  is the force vector (per unit volume).

The total F force (per unit volume), is represented as follows (Massel et al., 1999).

1. Upper layer:  $-(h-h_l) < z < 0$

$$\bar{F}_u = \frac{1}{2} \rho \bar{D}_u \sum_{j=1}^{j=N_u} C_d^{(m)}(\text{Re}) \bar{u}_{n,j}(x,z) |\bar{u}_{n,j}(x,z)| \quad (4)$$

2. Lower layer:  $-h < z < (h - h_l)$

$$\bar{F}_l = \frac{\rho \bar{D}_l}{2 \cos(\Theta)} \sum_{j=1}^{j=N_l} C_d^{(m)}(\text{Re}) \bar{u}_{n,j}(x,z) |\bar{u}_{n,j}(x,z)| \quad (5)$$

$\bar{u}_{n,j}$  is the velocity vector normal to the longitudinal axis of the particular trunk  $j$  induced by wave orbital velocity  $\bar{u}(x,z) = [u(x,z), w(x,z)]$ .  $\bar{D}_u$  and  $\bar{D}_l$  are the mean diameters of trunks in upper and lower layers, respectively, and  $\Theta$  is the inclination angle of trunks and roots in lower layer.  $C_d^{(m)}$  is modified drag coefficient which is function of the Reynolds number  $\text{Re}$ . The modified drag coefficient is given by

$$C_d^{(m)}(\text{Re}, x, z) = C_d(\text{Re}, x, z) K_i(N, \text{Re}), \quad (6)$$

in which  $K_i(N, \text{Re})$  is a modification factor which depends on mangrove density, i.e. number of trunks per unit area,  $N$  and  $\text{Re}$ .  $C_d(\text{Re}, x, z)$ , is given by (SPM, 1984)

$$C_d = \begin{cases} 1,2 & \text{for } \text{Re} \leq 2 \times 10^5 \\ 1,2 - 0,5 < \frac{\text{Re}}{3 \times 10^5} - \frac{2}{3} & \text{for } 2 \times 10^5 \leq \text{Re} \leq 5 \times 10^5 \\ 0,7 & \text{for } \text{Re} > 5 \times 10^5 \end{cases} \quad (7)$$

Determination of factor  $K_i$  is described in Appendix A of Massel et al. 1999.

Using equations (4) and (5), equation (3) can be written as

$$\frac{\partial \bar{u}_2}{\partial t} = \begin{cases} \frac{1}{\rho} \nabla(p_2 + \rho g z) - \frac{1}{\rho} \bar{F}_u(x,z), & -(h - h_l) < z < 0 \\ \frac{1}{\rho} \nabla(p_2 + \rho g z) - \frac{1}{\rho} \bar{F}_l(x,z), & -h < z < -(h - h_l) \end{cases} \quad (8)$$

Equation (8) is non linear equation due to non linearity of  $\bar{F}$  as shown in equations (4) dan (5). An analytical solution of Eq. (8) is possible after its linearization, i.e. replacing non linear term by the linear one such that the mean error ( $\bar{\varepsilon}$ ) of the substitution become minimal

$$\frac{1}{\rho} \bar{F}(x,t) \approx f_e \omega_p \bar{u}_2(x,z), \quad (9)$$

and

$$\bar{\varepsilon}(x, z) = \frac{1}{\rho} \bar{F}(x, z) - f_e \omega_p u_2(x, z) \rightarrow \text{minimum}$$

The linearization coefficient  $f_e$  can be evaluated from the minimalization, in the stochastic sense. The details of linearization procedure and determination of the coefficient  $f_e$  are given in Appendix B of Massel et al. 1999. The linearization coefficient is given as

$$f_e = \frac{1}{\omega_p} \sqrt{\frac{2}{\pi}} \left\{ \frac{\int_0^l \int_{-h}^{-(h-h_1)} \bar{D}_l N_l C_d^{(m)}(\text{Re}, x, z) \sigma_{u_2}^3 dx dz}{\int_0^l \int_{-h}^0 \sigma_{u_2}^2 dx dz} + \frac{\int_0^l \int_{-(h-h_1)}^0 \bar{D}_u N_u C_d^{(m)}(\text{Re}, x, z) \sigma_{u_2}^3 dx dz}{\int_0^l \int_{-h}^0 \sigma_{u_2}^2 dx dz} \right\} \quad (10)$$

Substituting equation (9) into equation (3) gives

$$\frac{\partial \bar{u}_2}{\partial t} = -\frac{1}{\rho} \nabla(p_2 + \rho g z) - f_e \omega_p \bar{u}_2 \quad (11)$$

Equation (11) is used to develop the velocity potential function  $\phi_2(x, z, t)$  for Region II. The velocity  $\bar{u}_2$  and pressure  $p_2$  are the wave-induced quantities which periodic in time i.e.,

$$\bar{u}_2 = |\bar{u}_2| \exp(-i\omega t), p_2 = |p_2| \exp(-i\omega t) \quad (12)$$

Thus, equation (11) becomes

$$\frac{1}{\rho} \nabla(p_2 + \rho g z) = \omega \left( -i - f_e \frac{\omega_p}{\omega} \right) \bar{u}_2 \quad (13)$$

Application of the operation curl  $A = \nabla x A$  to both sides of equation (13) yields

$$\omega \left( i - f_e \frac{\omega_p}{\omega} \right) \nabla x \bar{u}_2 = \frac{1}{\rho} \nabla x \nabla(p_2 + \rho g z) = 0 \quad (14)$$

Therefore,

$$\nabla x \bar{u}_2 = 0 \quad (15)$$

which indicates irrotationality and implies velocity potential exist, such that

$$\bar{u}_2 = \nabla \phi \quad (16)$$

Equation (15) and (16) yields

$$\nabla^2 \phi_2 = 0 \quad (17)$$

Using (16), equation (11) can be written as

$$\frac{\partial \phi_2}{\partial t} + \frac{1}{\rho}(p_2 + \rho g z) + f_e \omega_p \phi_2 = 0 \quad (18)$$

Equation (18) is a linearized Bernoulli equation of wave motion in Region II.

At the sea surface ( $z = \zeta$ ) and  $p = 0$ , equation (18) yields

$$\frac{\partial \phi_2}{\partial t} + g \zeta + f_e \omega_p \phi_2 = 0 \quad (19)$$

Considering the periodicity of the wave motion and the kinematic condition at the sea surface it is obtained

$$g \frac{\partial \phi_2}{\partial z} - \omega^2 \left( 1 + i f_e \frac{\omega_p}{\omega} \right) \phi_2 = 0 \text{ at } z = \zeta = 0 \quad (20)$$

By assuming the bottom is permeable gives

$$\frac{\partial \phi_2}{\partial z} = 0 \text{ at } z = -h. \quad (21)$$

Equations (16), (20) and (21) formulate the boundary value problem for velocity potential  $\phi_2$ . Coefficient  $f_e$  is determined through linearization.

To define the velocity potential  $\phi_2$  it should be noted that within the mangrove area, except for the progressive waves and waves reflected from the edge  $x = l$ , a set of disturbances will be present. These disturbances attenuate with the distance from both boundaries ( $x = 0$  and  $x = l$ ). Therefore, the velocity potential for wave motion within the mangrove forest takes the form (Massel et al., 1999)

$$\Phi_2(x, z, t) = \Re \int_{-\infty}^{\infty} \frac{g \exp(-i\omega t)}{\omega \left( i - f_e \frac{\omega_p}{\omega} \right)} \times \sum_{\psi} \left\{ \left[ P_{\psi} \exp(-\psi x) + Q_{\psi} \exp(\psi x) \right] \frac{\cos \psi(z+h)}{\cos \psi h} \right\} dA_1(\omega) \quad (22)$$

in which  $P_{\psi}$  and  $Q_{\psi}$  are the amplification factors of the spectral components propagating in positive and negative direction of the x-axis respectively. The complex wave number  $\psi$  has to satisfy of the following dispersion relation

$$\omega^2 \left( 1 + i f_e \frac{\omega_p}{\omega} \right) + g \psi \tan(\psi h) = 0. \quad (23)$$

In general, the wave number  $\psi$  is a complex function, i.e.  $\psi = \psi_r + i\psi_i$ . Real part,  $\psi_r$ , controls the attenuation of wave amplitude within the mangrove region and imaginary part,  $\psi_i$ , provide the phase of the wave. In the case where there is no energy dissipation, i.e.  $f_e = 0$  wave number  $\psi \rightarrow \alpha$ .

Behind the mangrove forest (Region III :  $x > l$ ;  $-h < z < 0$ ), we assume that only progressive waves, propagating out of the mangrove forest exist. Therefore, the velocity potential  $\phi_3$  takes the form

$$\Phi_3(x, z, t) = \Re \int_{-\infty}^{\infty} \left( \frac{-ig \exp(-\omega t)}{\omega} \right) \times \sum_{\alpha} T_{\alpha} \exp[\alpha(l-x)] \frac{\cos \alpha(z+h)}{\cos \alpha h} dA_i(\omega). \quad (24)$$

To calculate the unknown coefficients  $M_{\alpha}$ ,  $T_{\alpha}$ ,  $P_{\psi}$  and  $Q_{\psi}$ , the boundary conditions at  $x = 0$  and  $x = l$  are used, i.e., the potential  $\Phi_1(x, z, t)$ ,  $\Phi_2(x, z, t)$  and  $\Phi_3(x, z, t)$  must satisfy the matching conditions which provide continuity of pressure and horizontal velocity.

The velocity potential of the waves reflected from the mangrove forest can be presented as

$$\Phi_{1r}(x, t) = \Re \int_{-\infty}^{\infty} \frac{-ig}{\omega} \exp(-i\omega t) \sum_{\alpha} \tilde{M}_{\alpha} e^{\alpha x} \frac{\cos \alpha(z+h)}{\cos \alpha h} dA(\omega) \quad (25)$$

in which

$$\tilde{M}_{\alpha} = \begin{cases} M_k - 1 & \text{at } \alpha = -ik \\ M_{\alpha} & \text{at } \alpha \neq -ik \end{cases} \quad (26)$$

Thus, the surface elevation of reflected waves is

$$\zeta_{1r}(x, t) = \Re \int_{-\infty}^{\infty} e^{-i\omega t} \sum_{\alpha} \tilde{M}_{\alpha} e^{\alpha x} dA(\omega) \quad (27)$$

and frequency spectrum  $S_r(\omega, x)$  for waves reflected from the mangrove forest takes the form

$$S_r(\omega, x) = \left| \sum_{\alpha} \tilde{M}_{\alpha} e^{\alpha x} \right|^2 S_i(\omega). \quad (28)$$

Because of the presence of the evanescent modes (when  $\alpha \neq -ik$ ), the spectrum  $S_r(\omega, x)$  depends on the distance from a mangrove forest. However, at a sufficiently large distance from the mangrove forest, these modes disappear



completely and only reflected progressive waves (when  $\alpha = -ik$ ) are observed. Taking the limit  $x \rightarrow -\infty$  in Eq. (28) gives

$$S_r(\omega, x)_{x \rightarrow -\infty} = |M_k(\omega) - 1|^2 S_i(\omega). \quad (29)$$

In a similar way we find that the spectrum of waves transmitted through the mangrove forest becomes

$$S_t(\omega, x)_{x \rightarrow \infty} = |T_k(\omega)|^2 S_i(\omega). \quad (30)$$

The spectra (29) and (30) should be used to evaluate the reflection and transmission coefficients  $K_r$  and  $K_t$ . Taking the analogy to monochromatic waves we adopt the following expressions for the global reflection coefficient  $K_r$  and transmission coefficient  $K_t$

$$K_r = \frac{\sigma_r}{\sigma_i} = \frac{\left\{ \int_0^\infty S_r(\omega) d\omega \right\}^{1/2}}{\left\{ \int_0^\infty S_i(\omega) d\omega \right\}^{1/2}} \quad (31)$$

and

$$K_t = \frac{\sigma_t}{\sigma_i} = \frac{\left\{ \int_0^\infty S_t(\omega) d\omega \right\}^{1/2}}{\left\{ \int_0^\infty S_i(\omega) d\omega \right\}^{1/2}}, \quad (32)$$

in which  $S_i(\omega)$ ,  $S_r(\omega)$  and  $S_t(\omega)$ , are the incident, reflected and transmitted wave spectra, respectively. The  $\sigma_r$ ,  $\sigma_r$  and  $\sigma_i$  are the corresponding standard deviations. Conservation of wave energy requires that the following energy balance should be satisfied

$$E_r + E_t + E_{dis} = E_i \quad (33)$$

or

$$\sigma_i^2 = \sigma_r^2 + \sigma_t^2 + \sigma_{dis}^2 \quad (34)$$

Thus

$$K_r^2 + K_t^2 + K_{dis}^2 = 1 \quad (35)$$

in which  $K_{dis}$  is an energy dissipation coefficient.

### 3 Examples of Numerical Calculations

#### 3.1 Very Dense Mangrove Forest

##### 3.1.1 *Rhizophora* Species

Let us assume the following parameters of the mangrove forest: forest width  $l = 50$  m, water depth  $h = 1$  m, number of trunks in upper layer  $N_u = 16/\text{m}^2$ , number of trunks in lower layer  $N_l = 49/\text{m}^2$ , mean diameter of upper layer trunks  $\bar{D}_u = 0.08$  m and mean diameter of lower layer trunks  $\bar{D}_l = 0.02$  m.

The mangrove forest is subjected to wind induced waves characterized by a typical spectrum for shallow water (Massel et al., 1996)

$$S(\omega) = \frac{\sigma_\zeta^2}{\omega_p} \left\{ 1.835 \exp \left[ -22.222 \left( \frac{\omega}{\omega_p} - 1 \right)^2 \right] + 4.211 \left( \frac{\omega}{\omega_p} \right)^{-5} \exp \left[ -7.987 \left( \frac{\omega}{\omega_p} \right)^{-8} \right] \right\} \quad (36)$$

where  $\sigma_\zeta = H_s/4$ ,  $H_s$  is the significant wave height, and  $\omega_p$  is the peak frequency. In the calculations,  $H_s = 0.6$  m and  $\omega_p = 2\pi/5$ ; this means that the wave period  $T_p$  corresponding to  $\omega_p$  is  $T_p = 5$  s.

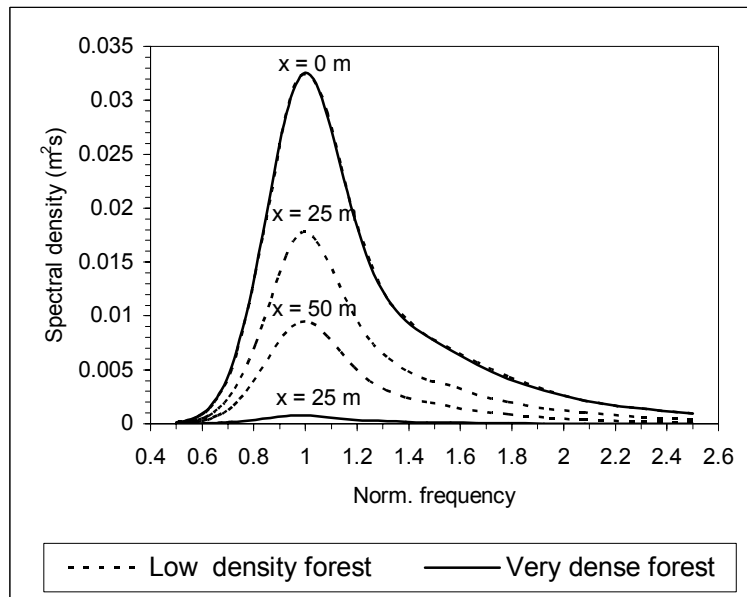


**Figure 2** Wave spectrum at three cross-section ( $x = 0, 25, 50$  m) in densely and sparsely populated forests.

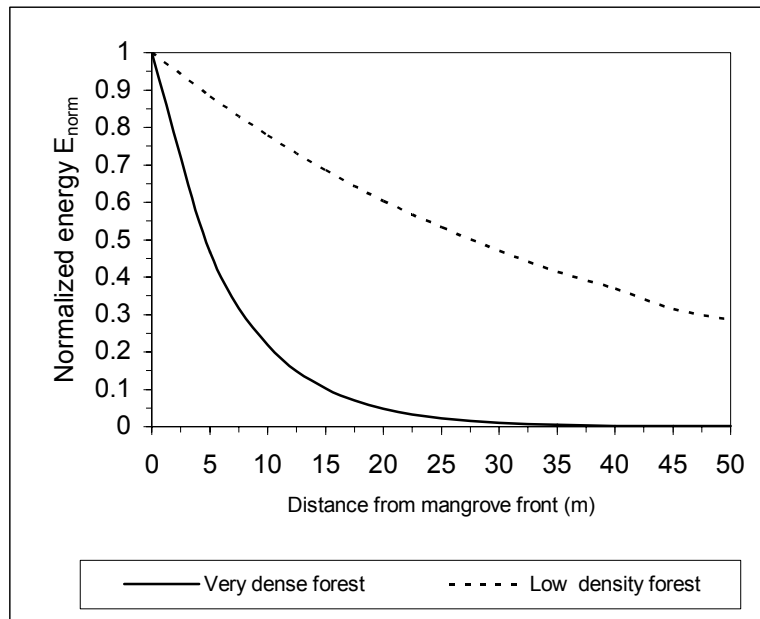


**Figure 3** Normalized energy  $E_{norm}$  in densely and sparsely populated forests.

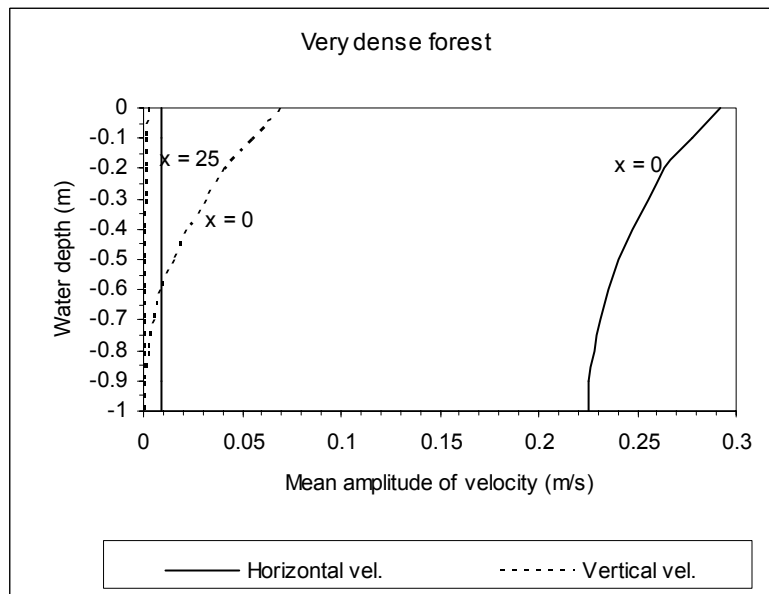


**Figure 4** Vertical profiles of the mean amplitudes of horizontal and vertical components of orbital velocity at cross-sections ( $x = 0, 25, 50$  m) in densely populated forest.

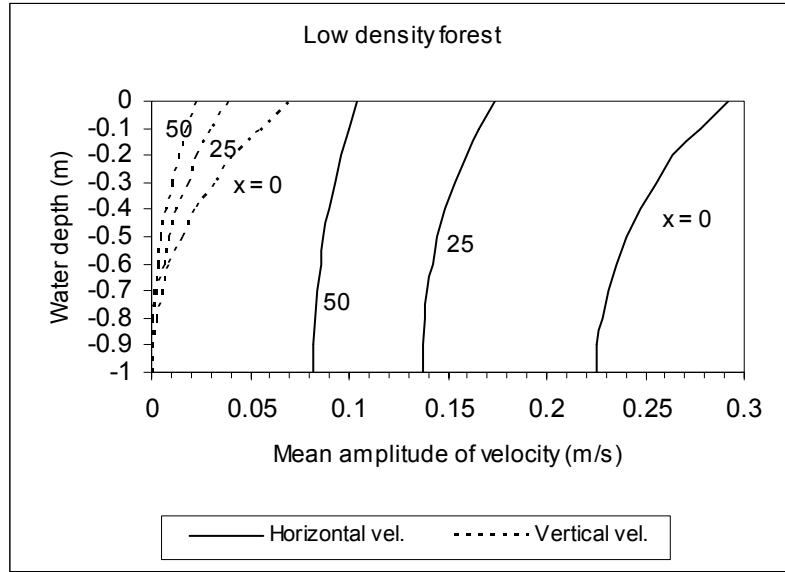


**Figure 5** Vertical profiles of the mean amplitudes of horizontal and vertical components of orbital velocity at cross-sections ( $x = 0, 25, 50$  m) in sparsely populated forest.

Numerical calculations indicate that for a given incident wave spectrum and given mangrove density the linearization coefficient  $f_e = 0.307$ . The reflection and transmission coefficient  $K_r$  and  $K_t$  are 0.07 and 0.03, respectively; it means that 99% of energy is dissipated within mangrove forest. This is confirmed also Fig. 2, in which the frequency spectra at three cross-sections in the mangrove forest are shown. Wave energy attenuates very fast with the distance from the mangrove front and behind the mangrove forest the wave energy is negligibly small.

Fig. 3 illustrates the normalized energy as a function of distance from mangrove front

$$E_{norm}(x) = \frac{\sigma_{\zeta}^2(x)}{\sigma_{\zeta}^2}. \quad (37)$$

In which  $\sigma_{\zeta}^2(x)$  represents wave energy at a distance  $x$  from the mangrove front and  $\sigma_{\zeta}^2$  is the incident wave energy.

Wave-induced velocities in mangrove forest are of special interest, as water kinematics control the exchange of water, fluxes of nutrients and sediments in mangrove. Both water velocity components change their direction during wave

period, however, for practical applications, the most useful characteristics of wave velocity is the mean amplitude. Under the assumption that both components of the wave-induced velocity are random quantities with the normal probability density, for mean amplitude of the horizontal ( $u$ ) and vertical ( $w$ ) velocity components we obtain:

$$\bar{u} = \sqrt{\frac{2}{\pi}} \sigma_u \quad \text{and} \quad \bar{w} = \sqrt{\frac{2}{\pi}} \sigma_w \quad (38)$$

in which  $\sigma_u$  and  $\sigma_w$  are the standard deviations of the horizontal and vertical velocity components, respectively. The vertical profiles of mean amplitudes  $\bar{u}$  and  $\bar{w}$  at the cross-section in a mangrove forest are shown in Fig. 4. In this case, the ratio of wavelength to water depth is relatively large,  $L/h = 16$  and the profiles of both velocity components are almost vertically uniform. They attenuate very quickly with distance from the mangrove front, and behind the mangroves they are negligible.

### 3.1.2 *Cerriops* Species

In this case, let us assume the following parameters of the mangrove forest: forest width  $l = 50$  m, water depth  $h = 1$  m, number of trunks in upper layer same as number of trunks in lower layer, i.e.,  $N_u = N_l = 16/\text{m}^2$  and  $49/\text{m}^2$ , mean diameter of upper layer trunks same as mean diameter of lower layer trunks, i.e.,  $\bar{D}_l = \bar{D}_u = 0.08$  m.

Numerical calculations indicate that for a given incident wave spectrum and mangrove density is  $16/\text{m}^2$  the linearization coefficient  $f_e = 0.3761$ . The reflection and transmission coefficient  $K_r$  and  $K_t$  are 0.089 and 0.018, respectively; it means that 99.59% of energy is dissipated within mangrove forest. Whereas for mangrove density is  $49/\text{m}^2$  the linearization coefficient  $f_e = 0.6951$ . The reflection and transmission coefficient  $K_r$  and  $K_t$  are 0.147 and 0.001, respectively; it means that 98.91% of energy is dissipated within mangrove forest. This is confirmed also Fig. 6, in which the frequency spectra at three cross-sections in the mangrove forest are shown. Wave energy attenuates very fast with the distance from the mangrove front and behind the mangrove forest the wave energy is negligibly small.

Fig. 7 illustrates the normalized energy as a function of distance from mangrove front. The vertical profiles of mean amplitudes  $\bar{u}$  and  $\bar{w}$  at the cross-section in a mangrove forests with density  $16/\text{m}^2$  and  $49/\text{m}^2$  are shown in Fig. 8 and 9 respectively. All of these figures also confirm that wave energy attenuates very fast with the distance from the mangrove front and behind the mangrove forest the wave energy is negligibly small.

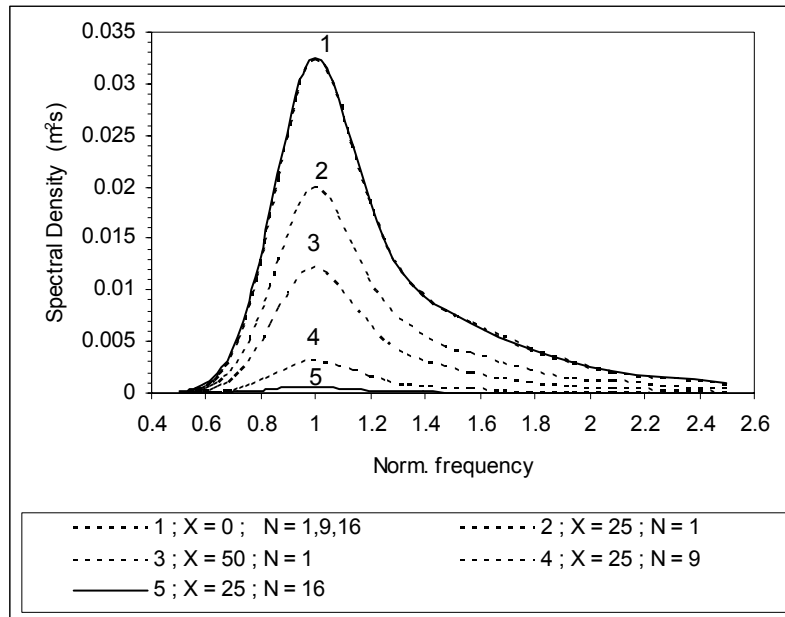


**Figure 6** Wave spectrum at three cross-section ( $x = 0, 25, 50$  m) in densely and sparsely populated forests for *Ceriops* species with trunk diameter is 0.08m.

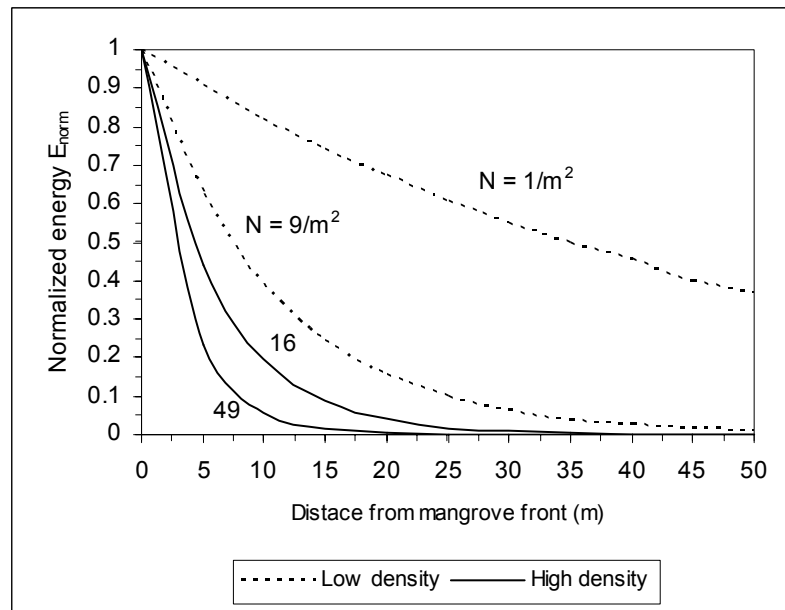


**Figure 7** Normalized energy  $E_{norm}$  in densely and sparsely populated forests for *Ceriops* species with trunk diameter is 0.08 m.

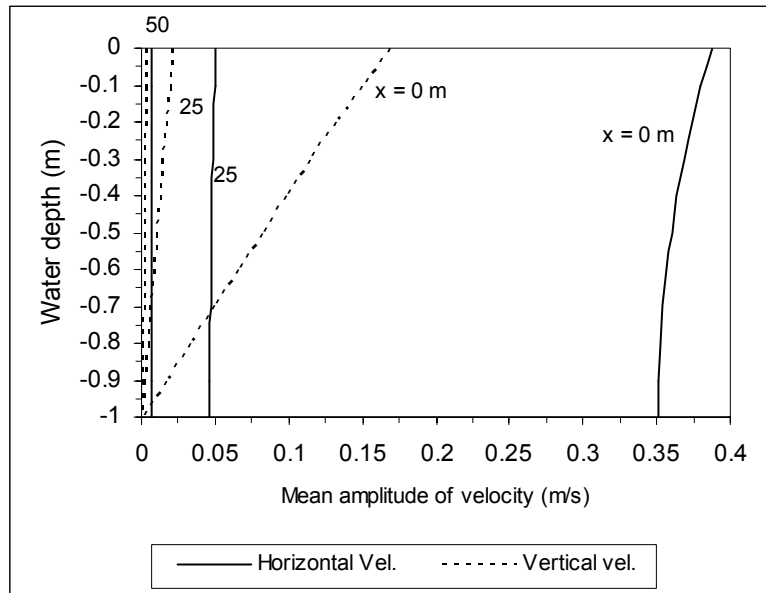


**Figure 8** Vertical profiles of the mean amplitudes of horizontal and vertical components of orbital velocity at cross-sections ( $x = 0, 25, 50$  m) for *Ceriops* species with density is  $16/m^2$  and trunk diameter is  $0.08$  m.

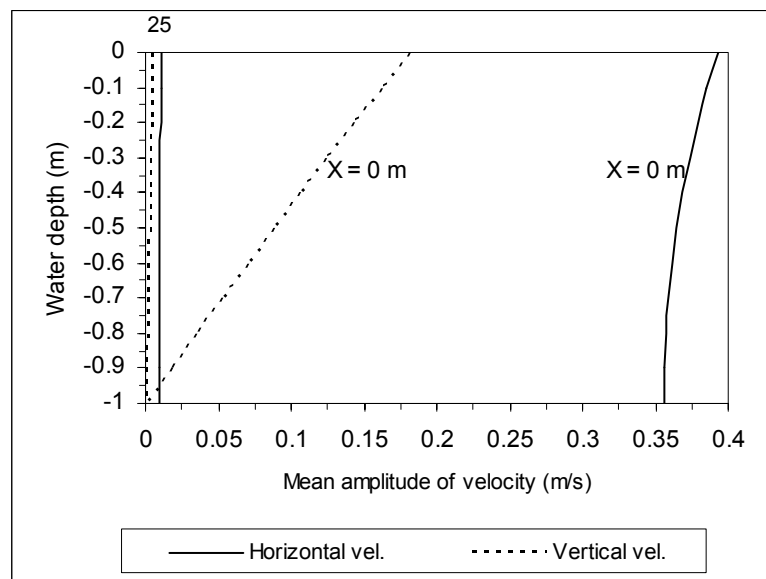


**Figure 9** Vertical profiles of the mean amplitudes of horizontal and vertical components of orbital velocity at cross-sections ( $x = 0, 25, 50$  m) for *Ceriops* species with density is  $49/m^2$  and trunk diameter is  $0.08$  m.

## 3.2 Mangrove Forest of Very Low Density

### 3.2.1 *Rhizophora* Species

In contrast to the above case, the mangrove forest is now sparsely populated by trunks, i.e.  $N_u = 1/\text{m}^2$  and  $N_l = 9/\text{m}^2$ . The other parameters of the mangrove forest and wave motion are the same as in case 3.1. The results of calculations are presented in Fig. 2, 3, and 5. In this case, wave energy is transmitted relatively easily through the mangrove forest with transmission coefficient  $K_t = 0.51$ . However, about 86% of energy is still dissipated by the mangrove. It should be noted that the linearization coefficient  $f_e$  is equal now 0.055.

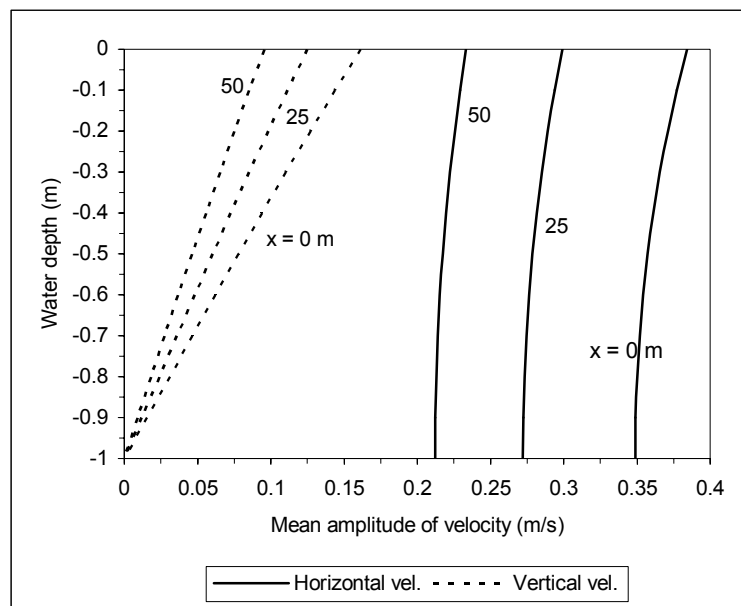


**Figure 10** Vertical profiles of the mean amplitudes of horizontal and vertical components of orbital velocity at cross-sections ( $x = 0, 25, 50$  m) for *Ceriops* species with density is  $1/\text{m}^2$  and trunk diameter is 0.08 m.

### 3.2.2 *Ceriops* Species

In this case, the mangrove forest is sparsely populated by *Ceriops* species with trunk density is  $N = 1/\text{m}^2$  and  $9/\text{m}^2$  and trunk diameters is 0.08 m. The other parameters of the mangrove forest and wave motion are the same as in the above case. The results of calculations are depicted in Fig. 6, 7, 10, and 11. Numerical calculations indicate that for a given incident wave spectrum and mangrove density is  $1/\text{m}^2$  the linearization coefficient  $f_e = 0.0451$ . The reflection and transmission coefficient  $K_r$  and  $K_t$  are 0.023 and 0.609, respectively; it



means that 79.28% of energy is dissipated within mangrove forest. Whereas for mangrove density is  $9/\text{m}^2$  the linearization coefficient  $f_e = 0.2131$ . The reflection and transmission coefficient  $K_r$  and  $K_t$  are 0.054 and 0.098, respectively; it means that 99.37% of energy is dissipated within mangrove forest. This is again confirmed that wave energy attenuates very fast with the distance from the mangrove front and behind the mangrove forest the wave energy is negligibly small.

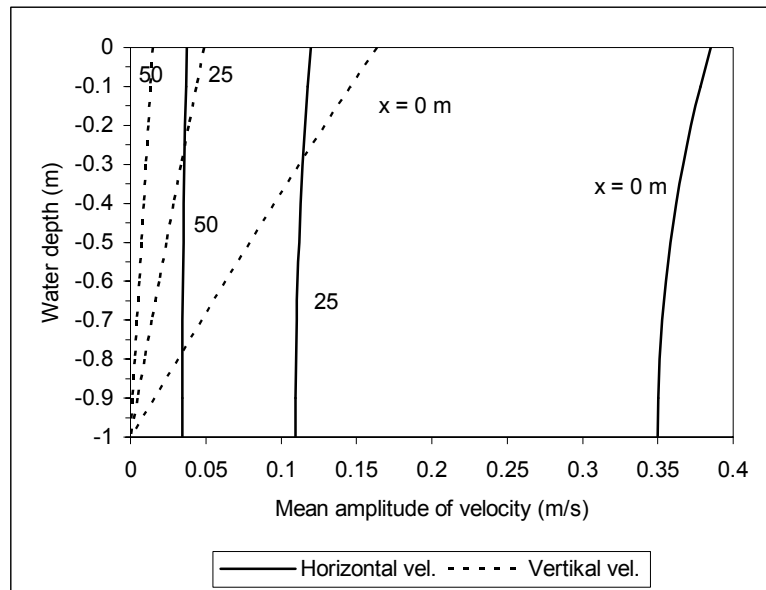


**Figure 11** Vertical profiles of the mean amplitudes of horizontal and vertical components of orbital velocity at cross-sections ( $x = 0, 25, 50$  m) for *Ceriops* species with density is  $9/\text{m}^2$  and trunk diameter is 0.08 m.

#### 4 Conclusions

This paper has presented the theoretical attempt to predict the attenuation of wind induced random waves in the mangrove forest. Two species of mangrove forest were investigated in this study i.e. *Rhizophora* and *Ceriops* forests. The energy dissipation in the frequency domain is determined by treating the mangrove forest as a random media with certain characteristics determined using the geometry of mangrove trunks and their locations. Resulting rate of wave energy attenuation strongly depends on the density of mangrove forest, diameter of mangrove roots and trunks, and on the spectral characteristics of the incident waves. Due to their roots *Rhizophoras* exhibit better capability in attenuating wave energy than *Ceriops*. Nevertheless densely populated *Ceriops* still effective in reducing wave energy. The analytical model of Massel et al.

1999 can be used as tool to give rough estimate on how thick the Rhizophora or Ceriops forests should be if we want to attenuate wave energy, at certain location, says 70% - 90%. This will help in designing the appropriate thickness of green belt in coastal areas.

### Acknowledgement

The authors would like to thank The Directorate General of Higher Education for providing a grant (Hibah Bersaing IX) in completing this research.

### List of Symbols

$\zeta$	=	water elevation
$\varepsilon$	=	Error
$\omega$	=	angular frequency
$k$	=	wave number
$f$	=	Frequency
$\rho$	=	water density
$g$	=	Gravitation
$S(\omega)$	=	frequency spectrum
$\omega_p$	=	peak frequency
$h$	=	water depth
$x$	=	horizontal coordinate
$z$	=	vertical coordinate
$l$	=	width of mangrove forest
$\phi$	=	potential velocity
$t$	=	Time
$\Re$	=	real part of the complex function
$\Im$	=	imaginary part of the complex function
$\alpha$	=	complex wave number
$E[ ]$	=	Averaging
$S_i$	=	frequency spectrum of incident wave
$\delta()$	=	delta function
$M_\alpha$	=	amplification factor
$\bar{u}_2$	=	velocity vector induced by waves
$p$	=	dynamic pressure
$\bar{F}$	=	Force per unit volume
$N_u$	=	number of trunks per unit area in upper layer
$\bar{D}_u$	=	mean diameters of trunks in upper layer
$h_l$	=	thickness of lower layer
$h_u$	=	thickness of upper layer

$N_i$	=	number of trunks per unit area in lower layer
$\bar{D}_l$	=	mean diameters of trunks in lower layer
$\Theta$	=	inclination angle of mangrove's trunks and roots
$F_d$	=	drag force
$V$	=	Volume
$A$	=	Area
$C_d$	=	drag coefficient
$Re$	=	Reynolds number
$C_d^{(m)}$	=	modified drag coefficient
$K_i$	=	modification factor
$f_e$	=	linearization coefficient
$\nabla$	=	delta operator
$P_\psi$	=	amplification factor of spectral component propagated in $x$ positive direction
$Q_\psi$	=	amplification factor of spectral component propagated in $x$ negative direction
$\psi$	=	complex wave number
$T_\alpha$	=	amplification factor
$\gamma$	=	wave number
$S_r$	=	frequency spectrum of reflected wave
$S_t$	=	frequency spectrum of transmitted wave
$\sigma_u$	=	standard deviation of horizontal velocity $u$
$\sigma_w$	=	standard deviation of vertical velocity $w$
$E_i$	=	incident wave energy
$E_r$	=	reflected wave energy
$E_t$	=	transmitted wave energy
$E_{dis}$	=	dissipated wave energy
$K_r$	=	reflection coefficient
$K_t$	=	transmission coefficient
$K_{dis}$	=	dissipation coefficient
$\sigma_j$	=	standard deviation of incident wave
$\sigma_r$	=	standard deviation of reflected wave
$\sigma_t$	=	standard deviation of transmitted wave
$\sigma_\zeta$	=	$\frac{H_s}{4}$
$\sigma_\zeta^2$	=	wave energy at a distance $x$ from the mangrove front
$\sigma_{\zeta_i}^2$	=	incident wave energy
$H_s$	=	significant wave height
$T$	=	wave period

$E_{norm}$  = normalized energy  
 $K_h$  = horizontal eddy viscosity

### References

1. Halide, H., Brinkman, R. M. & Ridd, P., *Designing Bamboo Wave Attenuators for Mangrove Plantations*, James Cook University, Townsville, Australia (2000).
2. Latief, H., Harada, K. & Imamura, F., *Experimental and Numerical Study on the Effect of Mangrove to Reduce Tsunami*, Tohoku University, Sendai, Japan (2000).
3. Latief, H., *Study on Tsunamis and their Mitigation by Using a Green Belt in Indonesia*, Dissertation, Tohoku University, Sendai, Japan (2000).
4. Massel, S. R., Furukawa, K. & Brinkman R. M., *Surface Wave Propagation in Mangrove Forests*, Fluid Dynamic Research, Elsevier Science, Amsterdam, vol. **24**, pp 219-249 (1999).
5. Massel, S. R., *Ocean Surface Waves: their Physics and Prediction*, World Scientific, Singapore, p.491 (1996).
6. Mazda, Y., Kanazawa, N. & Wolanski, E., *Tidal Asymmetry in Mangrove Creeks*. Hydrobiologia, Kluwer Academic Publishers, Belgium, vol. **295**, pp 51-58 (1995).
7. Miyagi, T., *Mangrove Habitat Dynamic and Sea-level Change*, Tohoku-Gakuin University, Sendai, Japan (1998).
8. SPM (*Shore Protection Manual*), Coastal Eng. Res. Center, U. S. Army Corps of Engineers, Washington, vol **I** (1984).